Elucidation of the Solution Conformations of Loloatin C by NMR Spectroscopy and Molecular Simulation

Heru Chen,[a] Richard K. Haynes,*[a] Jürgen Scherkenbeck,*[a,b] Kong H. Sze,[c,d] and Guang Zhu[c]

Keywords: Conformation analysis / Cyclic peptides / Molecular modelling / NMR spectroscopy

NMR experiments combined with molecular simulation with X-PLOR have been employed to determine the solution conformation of the cyclic decapeptide loloatin C in three different solutions. In DMSO, the molecule possesses a hydrophobic aromatic "wall" consisting of Trp^6 and Phe^7, and a type I β-turn structure involving Val^1, Trp^{10}, Asp^9 and Asn^8 with a hydrophobic head at Val^1/Trp^{10} and a hydrophilic tail at Asp^9 and Asn^8; another type II′ β-turn was also located between Leu^3, Tyr^4, Pro^5, and Trp^6. In 70/30 $[D_3]TFE/H_2O$, however, loloatin C possesses a dumbbell structure with all the hydrophobic side chains projecting upward on one side, forming a hydrophobic surface, and the hydrophilic side chains projecting to the other side, together with most of carbonyl oxygen atoms, thereby forming a hydrophilic surface. However, in 30:70 $[D_3]TFE/H_2O$, loloatin C possesses an inverse γ-turn incorporating Tyr^4, Pro^5, and Trp^6, a hydrophobic zone involving the side chains of Leu^3, Trp^6, Trp^{10}, and Phe^7 and a hydrophilic tail involving the hydrophilic side chains of Orn^2, Asn^8, and Asp^9. The amphiphilicity of the dumbbell structure in 70/30 $[D_3]TFE/H_2O$ is of interest in relation to the antibiotic activity of loloatin C.

Introduction

Loloatin C (**1**, Scheme 1) is a cyclic decapeptide containing two D-amino acids that was originally isolated from laboratory cultures of a tropical marine bacterium collected from the Great Barrier Reef at the southern coast of Papua New Guinea.[1] Because this compound exhibits potent antibiotic activity against several resistant Gram-positive and Gram-negative bacteria, it is a promising template to use for the development of new antibiotics. Through the total synthesis of loloatin C,[2] we have acquired milligram quantities of this compound. To establish a structure−function relationship, which will assist in the design and prediction of the properties of new members of this class,[3] we have carried out a study of the conformations of loloatin A. Because we were unable to crystallize the compound, we have used NMR, IR, and CD spectroscopies to elucidate its solution-state structures.

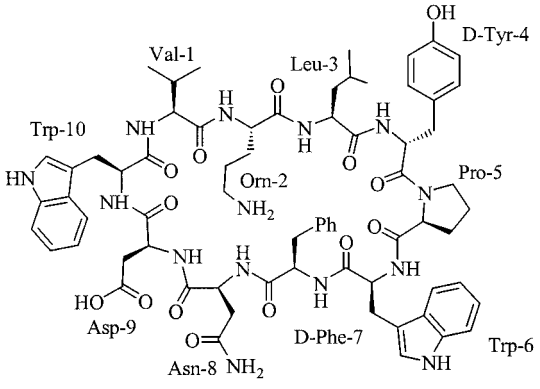

1: Loloatin C

Scheme 1

Recent developments in NMR spectroscopy have greatly enhanced our ability to obtain information on the three-dimensional structure of cyclic peptides,[4] especially when used in combination with molecular modelling in solution or in the crystalline state.[5,6] Several programs, such as CHARMM 24b2[7,8] and the CHARMM 23.1 force

[a] Department of Chemistry, The Hong Kong University of Science and Technology,
Clear Water Bay, Kowloon, Hong Kong, PR China
Fax: (internat.) + 852-2358-1594
E-mail: haynes@ust.hk
[b] Current affiliation:
Research Global Chemistry Insecticides, Bayer CropScience,
Alfred-Nobel Strasse 50, 40789 Monheim, Germany
Fax: (internat.) + 49-2173-383342
E-mail: juergen.scherkenbeck@bayercropscience.com
[c] Department of Biochemistry, The Hong Kong University of Science and Technology,
Clear Water Bay, Kowloon, Hong Kong, PR China
[d] Current affiliation:
Department of Chemistry, University of Hong Kong,
Pokfulam, Hong Kong, PR China

 DOI: 10.1002/ejoc.200300476

field,[9,10] have been used for molecular mechanics/dynamics calculations based on 2D and 3D NMR spectroscopic data. The Crystallization and NMR system (CNS) program X-PLOR[11] applies empirical energy functions combined with experimental data to allow exploration of the conformational space of macromolecules. We describe herein the elucidation of the three-dimensional conformation of loloatin C in different solvent systems through use of a combination of NMR spectroscopy and molecular simulation with X-PLOR.

Methodology

1D and 2D NMR spectroscopy experiments, including DQF-COSY,[12] total correlation spectroscopy (TOCSY),[13] and NOESY[14] were performed on a Varian Unity INOVA 500 MHz spectrometer. The raw data from the spectrometer were transformed into a data format readable by Sparky[15] in conjunction with the program NMRPipe.[16] The spin systems of loloatin C were assigned through the use of DQF-COSY, TOCSY, and NOESY spectra in conjunction with Sparky. The chemical shifts were then compiled into a shifts table and inserted into the data directory of the program X-PLOR. In this step, sequential NOEs together with easily identifiable NOEs were manually, but unambiguously, assigned; Sparky was utilized to assign unambiguously all the NOEs based on the shifts table. The NOE data were merged and transferred into a peaks table file. The shifts and peaks tables are the most important data in the program.

The vicinal coupling constant between the amide proton and α-proton, namely $^3J_{HN\text{-}H\alpha}$, was measured using the program PRONTO[17] based on the DQF-COSY spectrum, which implemented the Ludvigsen fitting procedure.[18] These data were translated into dihedral angles φ based on the Karplus equation.[19] The program ARIA[20,21] was employed to assign in iterative fashion useful but ambiguous NOEs. The routines were interfaced to X-PLOR. The manner is which X-PLOR was used for the structural simulation studies are described in the Exp. Sect.

Results and Discussion

NMR Spectroscopy and Structures

Three solvent systems — [D_6]DMSO, [D_3]TFE/H_2O (70:30), and [D_3]TFE/H_2O (30:70), designated as systems I, II, and III, respectively — were used. The spin systems of loloatin C in the three solvent systems were assigned exactly based on the methods described above. In Table 1 are listed the experimental values of the chemical shifts of the amide protons (HN) and the α-methine protons (Hα), and the values of the vicinal coupling constants, $^3J_{HN\text{-}H\alpha}$, which were acquired according to the procedure described above.

Table 1. Chemical shifts of the amide (HN) and α-methine protons (Hα) of loloatin C, and vicinal coupling constants $^3J_{HN\text{-}H\alpha}$ acquired from DQF-COSY (recorded at 25 °C, 500 MHz) in solvent systems I ([D_6]DMSO), II ([D_3]TFE/H_2O, 70:30), and III ([D_3]TFE/H_2O, 30:70)

	δHN (ppm)			δHα (ppm)			$^3J_{HN\text{-}H\alpha}$ (Hz)		
Residues	I	II	III	I	II	III	I	II	III
Val[1]	7.65	8.10	8.11	4.66	4.40	4.44	9.54	9.53	9.32
Orn[2]	8.97	8.12	8.24	5.39	5.34	5.34	11.7	5.78	10.4
Leu[3]	8.06	8.40	8.36	4.63	n.d.[a]	4.59	11.5	n.d.	9.98
D-Tyr[4]	9.28	8.27	8.42	4.30	4.27	4.24	6.48	12.0	3.41
Pro[5]	n.d.	n.d.	n.d.	4.11	4.11	4.16	n.d.	n.d.	n.d.
Trp[6]	7.30	7.69	7.71	4.57	4.66	4.66	11.8	8.38	7.67
D-Phe[7]	9.27	8.21	8.34	5.69	5.74	5.76	11.7	11.4	10.3
Asn[8]	9.14	9.25	9.28	4.30	4.89	4.90	9.56	7.76	7.44
Asp[9]	8.43	8.03	8.44	4.33	4.32	4.80	7.78	10.6	n.d.
Trp[10]	8.74	8.40	8.10	4.58	4.80	4.32	12.5	10.1	3.72

[a] n.d. = no data.

The chemical shifts of the amide protons vary in these different solvents. Solvent system I (DMSO) acts as a hydrogen bond acceptor for the amide protons; such hydrogen bonding causes a shift to higher field (lower chemical shift values) for the relevant amide protons. On the other hand, TFE is a hydrogen bond donor, and hydrogen bonding with the carbonyl oxygen atom induces shifts of the signals in the NMR spectrum of the neighboring amide proton to lower field.[22,23] The changes in chemical shifts of the amide protons in the residues Val[1], Leu[3], Trp[6], and Asn[8] that occur upon changing from solvent system I to solvent system II are consistent with these effects. However, the changes at the residues Orn[2], Tyr[4], Phe[7], Asp[9], and Trp[10] are in the opposite sense (Table 1); this situation is ascribed to the changes in conformation of loloatin C in the different solvent systems, as is discussed below.

Increasing the amount of water in TFE (systems II to III) also induces changes in the chemical shifts of the amide protons, as is shown clearly in Figure 1. The chemical shift that has the largest downfield change is that of Asp[9] (D9, $\Delta\delta = 0.412$ ppm). There are three moderate downfield

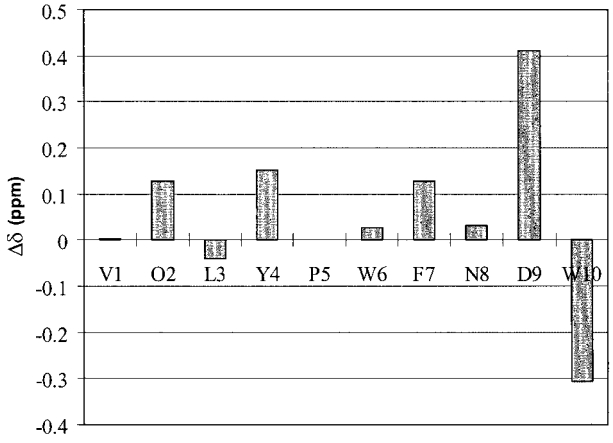

Figure 1. Difference in chemical shift of the amide protons between solvent systems II ([D_3]TFE/H_2O, 70:30) and III ([D_3]TFE/H_2O, 30:70), where $\Delta\delta = \delta_{III} - \delta_{II}$

changes: those of Orn[2] (O2), Tyr[4] (Y4), and D-Phe[7] (F7). The largest upfield shift is that for Trp[10] (W10, $\Delta\delta = -0.307$ ppm) and a small upfield change is observed for Leu[3] (L3). The chemical shifts of the amide protons of the other three residues are relatively similar in both solvent systems. Thus, loloatin C does display distinct structural differences in each of the solvent systems II and III.

In DMSO (solvent system I), the chemical shifts of the $C^{\alpha}H$ proton are an indicator of the secondary structure. An ensemble of several protons consistently having upfield shifts of ca. 0.3 ppm, relative to the standard values associated with a random coil, provides a strong indication for a helical structure. Conversely, an ensemble of several protons consistently having downfield shifts is indicative of the presence of β-strands.[24] According to Table 1, in solvent system I, the chemical shifts of the α-protons of residues Val[1] and Leu[3] display 0.31 and 0.25 ppm downfield shifts, respectively, relative to standard values, whilst that of Orn[2], when compared with the standard value of Lys, displays a downfield shift of 1.03 ppm. No data could be used to compare the chemical shift of the $C^{\alpha}H$ proton of the D-Phe[7] residue, although this proton appeared relatively downfield of other protons at $\delta = 5.69$ ppm. These data overall are indicative of a β-structure within residues 1−7, most likely a β-turn. On the other hand, the chemical shifts of the $C^{\alpha}H$ protons for Pro[5], Asn[8], and Asp[9] are located upfield of standard values by 0.33, 0.46, and 0.43 ppm, respectively. These data are indicative of a structure approximating an α-helix within residues 5−10. It must be borne in mind, however, that geometric constraints within the relatively small cyclic decapeptide will prevent it assuming a true α-helical structure, although a helical turn structure[25] can be expected.

No comments as to the possible secondary structures in systems II and III can be made at this stage, due to lack of standard data for the TFE/H_2O solvent systems.

The sensitivity of the chemical shifts of the amide protons to temperature (temperature gradients$\Delta\delta/T$) has been examined for solvent system III to probe the presence of intra- or intermolecular hydrogen bonds within the structure. The results are presented in Table 2. Only three of the values of $\Delta\delta/T$ for the amide protons, namely those of Val[1], Trp[6], and Trp[10], appear in the range from $2\cdot10^{-3}$ to $6\cdot10^{-3}$ ppm/K. This indicates that there may be hydrogen bonds between these protons and other atoms having greater electronegativity.

The number of unique NOESY cross peaks were identified for all the three systems, in which the spin lock mixing times (τ_m) were 1 s, 1 s, and 500 ms for solvent systems I, II, and III, respectively. There were 628, 380, and 247 unique cross peaks for solvent systems I, II, and III, respectively. Whilst it seems that the NOE intensities in system I are unreasonably large, a second NOESY experiment conducted at 750 MHz ($\tau_m = 100$ ms), in which the cross peak number is almost at the same level (651), rules out the possibility of spin diffusion during the high mixing time. Sequential constraints are displayed in Figure 2.

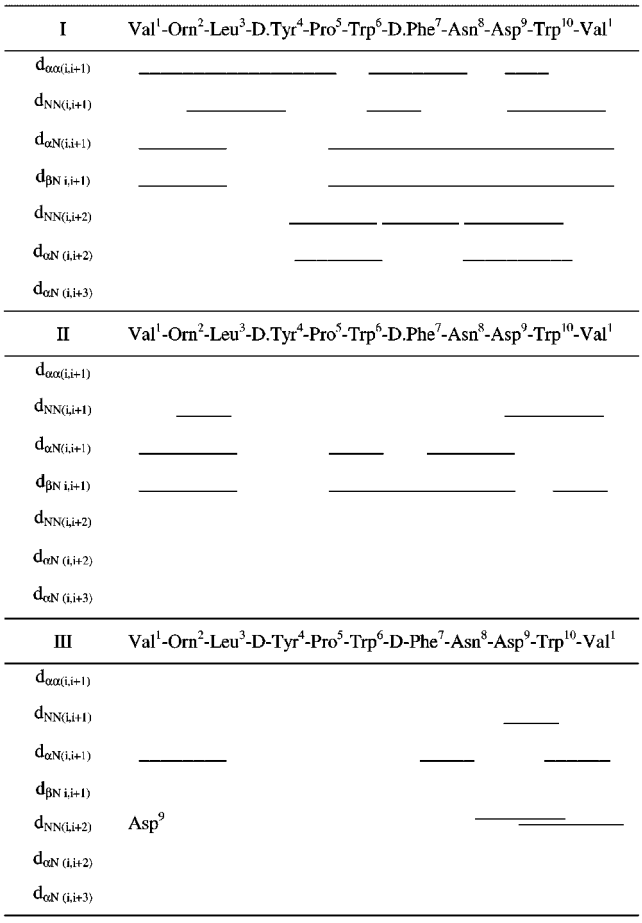

Figure 2. Schematic representation of the sequential and medium-range connectivities of loloatin C in solvent systems I ([D_6]DMSO), II ([D_3]TFE/H_2O, 70:30), and III ([D_3]TFE/H_2O, 30:70)

Table 2. Temperature gradients of the chemical shifts of amide protons in solvent system III ([D_3]TFE/H_2O, 30:70)

Temp. (K)	Val[1]	Orn[2]	Leu[3]	D-Tyr[4]	Trp[6]	D-Phe[7]	Asn[8]	Asp[9]	Trp[10]
283.5	8.08	8.12	8.29	8.36	7.67	8.24	9.20	8.34	8.04
288.5	8.11	8.21	8.37	8.38	7.69	8.31	9.26	8.43	8.09
293.5	8.11	8.24	8.36	8.42	7.71	8.34	9.28	8.44	8.1
298.5	8.14	8.29	8.38	8.47	7.74	8.36	9.32	8.48	8.13
303.5	8.17	8.38	8.43	8.52	7.76	8.40	9.36	8.54	8.15
313.5	8.20	8.38	8.46	8.55	7.80	8.40	9.39	8.56	8.17
$\Delta\delta/T \times 10^{-3}$ (ppm/K)	4.0	8.67	5.67	6.33	4.33	5.33	6.33	7.33	4.33

In solvent system I, $H^{\alpha}-H^{\alpha}$, $H^{\alpha}-H^{N}$, $H^{N}-H^{N}$, and $H^{\beta}-H^{N}$ connectivities are within Val^1 to Trp^{10} although some disconnectivities exist here and there. Short-range $H^{N}-H^{N}$ (i, $i+2$)-type connectivities are also identified between Tyr^4-Trp^6, Trp^6-Asn^8, and Asn^8-Trp^{10}; taken together with the identification of $H^{\alpha}-H^{N}$ (i, $i+2$)-type connectivities between Tyr^4-Trp^6 and Asp^9-Val^1, these indicate the existence of two turns within these regions.

Less structural information could be acquired from the analysis of NOE connectivities found in solvent systems II and III. The uncovering of $H^{N}-H^{N}$ (i, $i+2$)-type connectivities between Asn^8-Trp^{10} and Asp^9-Val^1 indicates the possible existence of a turn structure in solvent system III.

3D Solution Structure Determined by X-PLOR

Molecular simulation with X-PLOR version 3.851 was performed for the three solvent systems indicated above.

In Figure 3 is given the 3D solution structure of loloatin C in DMSO. Within the structure, two β-turn secondary structures are found. One is a type I β-turn between Val^1, Trp^{10}, Asp^9, and Asn^8 with a hydrogen bond of 2.741 Å between the Val^1 NH and the Asn^8 O atom, with an O−H−N angle of 112.83°. The other is a type II′ β-turn, which is located between Leu^3, Tyr^4, Pro^5, and Trp^6 with a hydrogen bond between the Leu^3 O atom and the Trp^6 NH unit (2.512 Å; 158.99°).

The backbone conformation displayed in Figure 3 approximates that of an antiparallel β-strand. A hydrophobic aromatic "wall" consisting of Trp^6 and Phe^7, and a type I β-turn structure involving Val^1, Trp^{10}, Asp^9 and Asn^8 with a hydrophobic "head' at Val^1/Trp^{10} and a hydrophilic "tail" at Asp^9/Asn^8 are apparent. As indicated in Table 3, the backbone dihedral angles ω in all cases are close to either +180° or −180°, which suggests that there are no *cis* elements in the backbone. There is a strong NOE between Trp^{10}HN and Val^1HN, i.e., the $d_{NN(i+2,i+3)}$ — the best diagnostic NMR spectroscopic parameter for identifying a type I β-turn structure — provides strong support for a type I β-turn structure between Val^1, Trp^{10}, Asp^9, and Asn^8. Another secondary structural element is a type II′ β-turn between Leu^3, Tyr^4, Pro^5, and Trp^6, which is apparent because of the presence of a strong NOE between δH(i+2) and HN(i+3). The torsion angles of the residues i+1 and i+2 presented in Table 3 also add support to the presence of the corresponding secondary structures, and the conclusion is consistent with the results from the NOESY analysis.

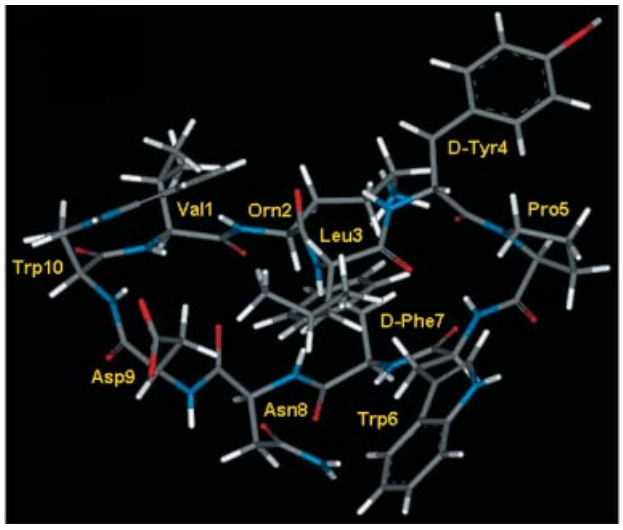

Figure 3. 3D structure of loloatin C in [D_6]DMSO based on a molecular simulation by X-PLOR

Structural simulation from data of solvent system II reveals a rather different structural arrangement. As is apparent from Figure 4, no intramolecular hydrogen bonds are observed within the molecule, and the overall shape approximates that of a dumbbell having an "intersection" point at Orn^2 and D-Phe^7. All the hydrophobic side chains project upward on one side, forming a hydrophobic surface. The hydrophilic side chains of the Orn^2, Asp^9, and Asn^8 residues project from the other side, together with most of the carbonyl oxygen atoms, which thereby form a hydrophilic surface. The backbone dihedral angles listed in Table 3 are consistent with this arrangement, i.e., all the amide bonds are in the *trans* form, as previously observed in solvent system I (DMSO). In all cases, the values of ω are ca. 180° or −180°. Evidence from the NOESY spectrum also supports the dumbbell structure: there are strong NOEs of $d_{\alpha\alpha(2,7)}$, corresponding to1.912 Å, and $d_{\alpha\delta(2,7)}$, corresponding to 1.766 Å, between Orn^2 and Phe^7.

Table 3. Backbone dihedral angles for the ensemble-average structure of loloatin C in solvent systems I ([D_6]DMSO), II ([D_3]TFE/H_2O, 70:30), and III ([D_3]TFE/H_2O, 30:70) determined by X-PLOR

Residues	φ I	φ II	φ III	ψ I	ψ II	ψ III	ω I	ω II	ω III
Val^1	−162.3	−62.0	−90.0	−42.5	−37.8	−39.8	−179.2	179.8	179.5
Orn^2	−170.4	59.3	−61.3	115.2	56.9	−33.4	179.4	−179.7	−179.5
Leu^3	−84.2	−59.2	−62.3	51.8	−45.0	140.1	−178.8	179.2	−179.6
D-Tyr^4	74.1	157.6	−64.1	−122.1	−53.9	−127.5	179.4	179.5	179.3
Pro^5	−61.0	−46.1	−72.1	−0.6	−42.1	51.9	−179.6	179.1	−178.6
Trp^6	−66.5	−162.0	−78.2	−140.0	−98.7	−53.1	179.0	−179.8	−178.8
D-Phe^7	176.8	74.7	51.7	56.5	123.2	102.3	176.9	−179.9	−178.4
Asn^8	−164.6	−85.5	−170.7	−143.5	−53.4	−32.1	179.7	−179.7	−178.7
Asp^9	−60.8	−165.7	−176.6	−38.8	34.6	−47.5	179.3	−179.3	−179.3
Trp^{10}	−79.5	−110.5	−71.3	0.56	−126.2	139.9	−179.8	−179.3	179.3

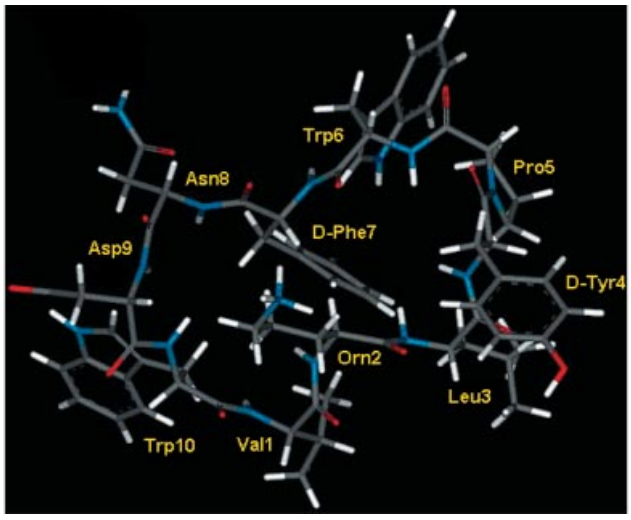

Figure 4. 3D structure of loloatin C in solvent system II ([D_3]TFE/H_2O, 70:30) based on a molecular simulation by X-PLOR incorporating the effect of water

In this specific conformation, therefore, there is an apparent amphiphilicity arising from lipophilic side chains projecting from one side and the hydrophobic chains projecting from the other side, a situation reminiscent of the "sidedness" displayed by gramicidin S. This feature appears to be an important one for maintaining high levels of antibiotic activity in analogues of gramicidin S.[26] Although the pronounced amphiphilicity of loloatin C is apparent only in the 70:30 [D_3]TFE/H_2O solvent system, the amphilicity does have an analogy with that of gramicidin S, and, thus, this particular solution state structure is of interest because of the potent antibiotic activities displayed by loloatin C.

Increasing the amount of water with respect to TFE, as in solvent system III ([D_3]TFE/H_2O, 30:70), induced a marked structural change from the dumbbell motif of solvent system II. The structure is given in Figure 5.

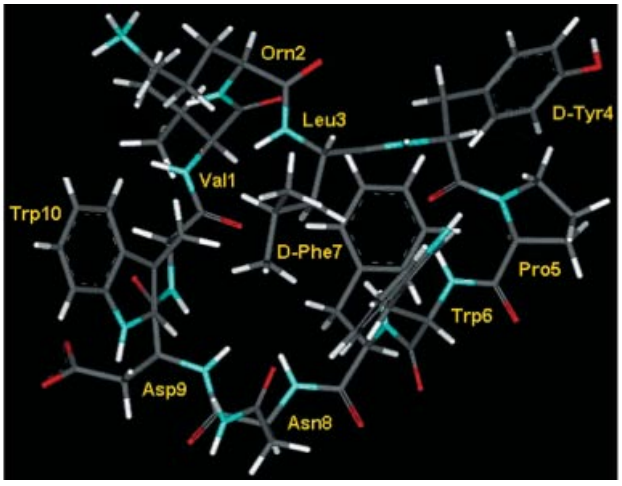

Figure 5. 3D structure of loloatin C in solvent system III ([D_3]TFE/H_2O, 30:70) based on a molecular simulation by X-PLOR incorporating the effect of water

Only one secondary structural type was found, namely the inverse γ-turn incorporating Tyr^4, Pro^5, and Trp^6 in which the hydrogen bond of 1.97 Å between the Tyr^4 O atom and the Trp^6 NH, with an O−H−N angle of 137.78°. The hydrophobic side chains of Leu^3, Trp^6, Trp^{10}, and Phe^7 are clustered together to form a hydrophobic zone (the "head") and the hydrophilic side chains of Orn^2, Asn^8, and Asp^9 form a hydrophilic "tail'. The ring is relatively constricted around Leu^3, Tyr^4, Pro^5, and Trp^6.

To illustrate the effectiveness of the convergence in the X-PLOR simulation, superpositions of 10 minimum energy structures of Loloatin C in the 30:70 [D_3]TFE/H_2O solvent system is presented in Figure 6. It is apparent that the structures converge well.

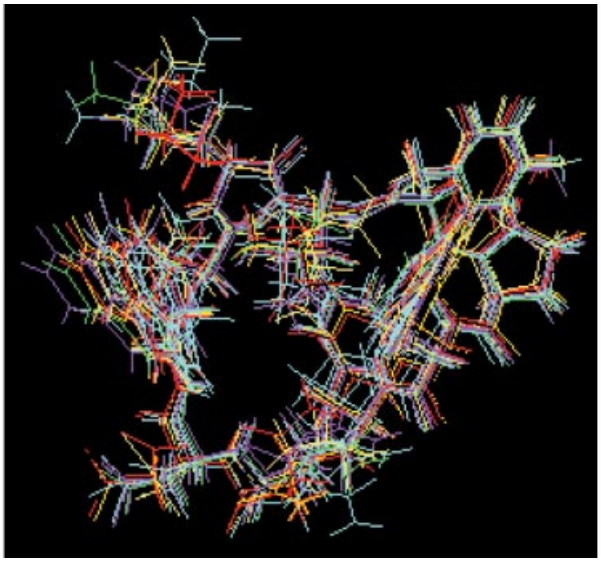

Figure 6. Superposition of 10 minimum-energy structures of loloatin C in solvent system III ([D_3]TFE/H_2O, 30:70) calculated by X-PLOR and displayed by molmol

Studying Circular Dichroism (CD)

CD was employed to check the 3D solution structure of loloatin C. We chose to use a solution of 30 wt-% trifluoroethanol (TFE) in 10 mM sodium acetate buffer as the medium on the basis that TFE acts as a structure-promoting, membrane-mimicking solvent.

In Figure 7 are displayed the curves. There is a positive band at 190 nm and negative bands at 204 and 217 nm. Thisis indicative of a blend of α-helix and β-turn structures. As indicated by the shape of the curves, and by an on-line deconvolution analysis using CDNN,[27] the domain conformation is believed to be a helix-like structure with a small component of a β-structure. This conformation is consistent with the results of the molecular simulation for solvent system III (TFE/H_2O, 30:70).

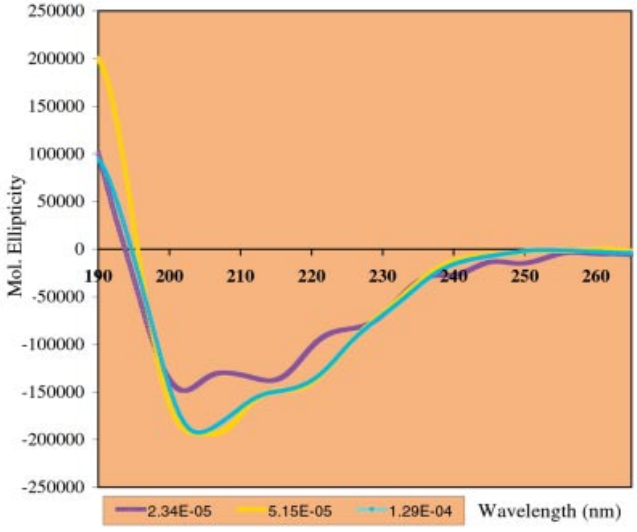

Figure 7. CD spectra of loloatin C in TFE/buffer (30 wt-% trifluoroethanol in 10 mM NaOAc, pH 5.5); concentrations are $2.34 \cdot 10^{-5}$ M for the maroon line, $5.15 \cdot 10^{-5}$ M for the yellow line, and $1.29 \cdot 10^{-4}$ M for the azure line

Conclusion

Based on the results obtained for the three solvent systems, it is apparent that the skeleton of loloatin C is relatively flexible, with quite pronounced changes in conformation taking place upon changes in the solvent. Thus, in a solvent like DMSO, which can act as a hydrogen bond acceptor, the inverse-turn secondary structure is stable, whereas in solvents that can act as hydrogen bond donors, such as TFE, the inverse-turn structures are destabilized. Of particular interest is the dumbbell-like conformation displayed by loloatin C in solvent system II ([D_3]TFE/H_2O, 70:30). In this specific conformation, the apparent amphiphilicity, due to lipophilic side chains projecting from one side and hydrophobic chains projecting from the other, is reminiscent of the "sidedness" displayed by gramicidin S. As this feature appears to play a role in maintaining high levels of antibiotic activity in analogues of gramicidin S, this particular solution state structure of loloatin C is of interest in regard to the potent antibiotic activities displayed by this compound.

Experimental Section

NMR Experiments: Loloatin C was dissolved in a suitable solvent (500 μL). Three solvent systems were employed: [D_6]DMSO, [D_3]TFE/H_2O (70:30) and [D_3]TFE/H_2O (30:70). In the [D_3]TFE/H_2O systems, 0.05 wt-% sodium 3-(trimethylsilyl)[2,2,3,3-D_4]propionate (TMSP) was added as the internal standard. The peptide concentration in [D_6]DMSO was 4 mM, in [D_3]TFE/H_2O (70:30) it was 2 mM, and in [D_3]TFE/H_2O (30:70) it was 1 mM.

The ^{1}H and one- and two-dimensional NMR spectroscopy experiments, including DQF-COSY, total correlation spectroscopy (TOCSY), and NOESY experiments were performed at 25 °C on a Varian Unity INOVA 500 spectrometer equipped with a triple resonance probe and a *z*-axis pulse-field gradient. One NOESY experiment, with a mixing time of 100 ms, was performed on a Unity INOVA 750 spectrometer equipped with a triple resonance probe and a *z*-axis pulse-field gradient. One-dimensional FIDs (free induction decays) were typically acquired through presaturation of the water signal using low-power irradiation, a sweep width of 12 ppm, and digitized into 6400 complex points. Two-dimensional data sets were acquired typically using a ^{1}H sweep width of 12 ppm and presaturation of the water signal into matrices of 4096 to 2048 complex data points in t_2 and 1024 to 2048 in t_1; the signal was averaged over 32 transients. Quadrature detection in F1 was achieved using the States-TPPI method.[28] For the TOCSY spectra, spin-lock mixing times of 70 ms for the DMSO system and 60 ms for the TFE/H_2O systems were applied for long-range through-bond connectivities. Shorter mixing times were not tried. Several NOESY spectra were recorded using mixing times (τ_m) between 100 ms and 1 s. Low-power (tpwr = 2) irradiation of the water signal was used during the mixing time of the NOESY spectra. Parameters used in the NOESY experiment with the 750 MHz spectrometer were as follows: t_2 = 4096; t_1 = 2048; *nt* = 32 transients; τ_m = 100 ms. The spectra were referenced relative to the chemical shift of methyl group (δ = 2.60 ppm) of DMSO when it was used as the solvent. For the TFE/H_2O system, the spectra were referenced relative to the chemical shift of methyl group in TMSP. This value was set to δ = 0. For the [D_3]TFE/H_2O (30:70) solvent system, temperature coefficients for the backbone amides were acquired. The measurements were carried out by acquiring 1D spectra in steps of 5 °C, between 10 and 40 °C, and by obtaining DQF-COSY and NOESY spectra at 15, 25, and 30 °C.

Structure Calculations: NOE volumes were integrated with SPARKY. Only the inter-residue NOEs were applied in the calculations. Structures were generated using simulated protocols published in the literature using the extended latest version (v. 3.851) of X-PLOR. To increase efficiency, modifications were introduced in the protocols to include the ambiguous distance restraints, floating assignment for prochiral groups and a reduced representation for non-bonded interactions for part of the calculation. The extensions of X-PLOR were necessary for the floating assignment approach used, the analysis and partial automatic assignment of the ambiguous NOEs and the best-fitting procedure. The parameters used in the refinement protocol were the same as those described in the literature.

Molecular simulations with X-PLOR (v. 3.851) were performed for the three NMR solvent systems indicated above. Before commencing the program, a sequence file — the LoC.seq file — was compiled to describe sequence of the peptide and it was included in the data directory of the program. The sequence is: Val−Orn−Leu−D-Tyr−Pro−Trp−D-Phe−Asn−Asp−Trp. Secondly, as loloatin C is a cyclic peptide containing an abnormal amino acid, namely ornithine, and two D-amino acids, D-phenylalanine, and D-tyrosine, some modifications are required. The parameters for ornithine were based on those of lysine, because there is only one methylene unit difference between them. These parameters were added to the file topallhdg5.2.pro of the database. Two allowances must be made for the cyclic structure. Firstly, it is necessary to insert comments on the first and last modifications of residues in the topallhdg.pep file for normal proteins. Secondly, a syntax for making cyclic peptides should be included in generate.inp, which is the file used for

creating the template for loloatin C. The syntax is: patch pept reference = "−" = (resid 10) reference = "+" = (resid 1) end

In this file, the syntax for changing the a normal L amino acid into a D amino acid is also included: patch ltod reference = nil = (resid 4) reference = nil = (resid 7) end

Also, an improper parameter should be included in the file parallhdg5.2.pro of the toppar directory. Otherwise, the change from an L to D configuration will not be effective. The syntax is as follows: IMPRoper CH2E N C HA 500.00 {sd = 0.031} 0 67.7957 IMPRoper CH2E NH1 C HA 500.00 {sd = 0.031} 0 66.1640

At this point, the molecular simulation is ready to start.

At the outset, the number of scanned structures (nstruct) in an iteration is set at 20, and keepstruct, the number of minimum-energy structures amongst the 20 raw structures is set at seven. Each run contains eight iterations. Later iterations are based on the results of the previous ones. The last iteration, i.e., the eighth, will analyze the structures retained in the previous iterations, and there will be several cycles to establish if the structural imputations are self-consistent. Manual examination of the assignments and the NOEs based on the simulation results can be carried out, and possible errors can be corrected at this stage. A larger-scale run with the commands nstruct = 60, keepstruct = 10, is then performed. When all the evaluations based on energy, NOE violation, and convergence are satisfied, the last is refined to include the effect of water molecules on the structure. In this manner, the final minimized structure was obtained. The 3D structures are displayed both by molmol[29] and TITAN (Wavefunction, Inc. and Schrödinger, Inc., USA). The molecular simulations were performed on a Linux platform.

Circular Dichoism (CD) Measurements: CD spectra were recorded on a Jasco J-720 spectropolarimeter. The instrument sample compartment was fitted with a cell holder that retained the sample cuvette near the photomultiplier tube to minimize light-scattering artifacts. The pathlength of the cell was 0.1 cm. The compartment and photomultiplier path were filled with high-purity N_2 (99.99%) to avoid the generation of ozone, which will otherwise substantially affect the spectra, especially in the near-UV range (180−200 nm). For each sample, blank solution and sample solution spectra were acquired simultaneously under identical conditions. The spectra were averaged from five scans at one gain and a spectral resolution of 0.1 nm for wavelengths from 190 to 265 nm. The true spectra for the samples were then derived by subtraction of the blank from the sample spectra. The ellipticity was recorded in terms of molar ellipticity. Spectra were recorded in 10 mM sodium acetate buffer (pH 5.5−6.0) containing 30 wt-% trifluoroethanol (TFE). Stock solutions were prepared by dissolving the corresponding fresh peptides in the corresponding solvent systems to a concentration of ca. $1 \cdot 10^{-4}$ M. Working solutions were prepared by sequential dilution of the stock solution by 5- to 10-fold.

Acknowledgments

We express our thanks to Bayer AG for their generous financial support of this work at the Hong Kong University of Science and Technology. Support from the Hong Kong University of Science and Technology Grant HKUST DAG01/02.SC10 is also gratefully acknowledged.

[1] J. M. Gerard, P. Haden, M. T. Kelly, R. J. Anderson, *J. Nat. Prod.* **1999**, *62*, 80−85.
[2] J. Scherkenbeck, H.-R. Chen, R. K. Haynes, *Eur. J. Org. Chem.* **2002**, 2350−2355.
[3] H. Neurath, R. L. Hill, in: *The Protein: The Three-Dimensional Structure of Cyclic Peptides and its Relation to Biological Function* (Eds.: H. Neurath, R. L. Hill), Academic Press, New York, London, **1982**, pp. 441−459.
[4] C. R. Cantor, V. T. Ivanov, H. Lis, Y. A. Ovchinnikov, N. Sharon, S. N. Timasheff, in: *The Protein* (Eds.: H. Neurath, R. L. Hill), 3rd Ed., Vol. V, Academic Press, New York, London **1982**, pp. 452−457.
[5] A. P. Tonge, P. Murray-Rust, W. A. Gibbons, L. K. McLachlan, *J. Comput. Chem.* **1988**, *9*, 522−538.
[6] C. McInnes, L. H. Kondejewski, R. S. Hodges, B. D. Sykes, *J. Biol. Chem.* **2000**, *275*, 14287−14294.
[7] F. Cárdenas, M. Thormann, M. Feliz, J.-M. Caba, P. Lloyd-Williams, E. Giralt, *J. Org. Chem.* **2001**, *66*, 4580−4584.
[8] B. R. Brooks, R. E. Bruccleri, B. D. Olafson, D. J. States, S. Swaminathan, M. J. Karplus, *J. Comput. Chem.* **1983**, *4*, 187−217.
[9] F. A. Momany, R. J. Rone, *J. Comput. Chem.* **1992**, *13*, 888−900.
[10] F. A. Momany, R. Rone, H. Kunz, R. F. Frey, S. Q. Newton, L. Schäfer, *Theochem.* **1993**, *286*, 1−18.
[11] A. T. Brunger, P. D. Adams, G. M. Clore, P. R. Gros, W. Grosse-Kunstleve, J.-S. Jiang, J. Kuszewski, N. Nilges, N. S. Pannu, R. J. Read, L. M. Rice, T. Simonson, G. L. Warren, *Acta Crystallogr. D* **1998**, *54*, 905−921.
[12] M. Rance, O. W. Sorensen, G. Bodenhausen, G. Wagner, R. R. Ernst, K. Wüthrich, *Biochem. Biophys. Res. Commun.* **1983**, *117*, 479−485.
[13] D. G. Davis, A. Bax, *J. Am. Chem. Soc.* **1985**, *107*, 2820−2821.
[14] J. Jeener, B. H. Meier, P. Bachmann, R. R. Ernst, *J. Chem. Phys.* **1979**, *71*, 4546−4553.
[15] T. D. Goddard, D. G. Kneller, *SPARKY 3*, University of California, San Francisco; unpublished work.
[16] F. Delaglio, S. Grzesiek, G. Vuister, G. Zhu, J. Pfeifer, A. Bax, *J. Biomol. NMR* **1995**, *6* 277−293.
[17] M. Kjar, K. V. Andersen, F. M. Poulsen, *Methods Enzymol.* **1994**, *239*, 288−308.
[18] S. Ludvigsen, K. V. Andersen, F. M. Poulsen, *J. Mol. Biol.* **1991**, *217*, 731−736.
[19] A. Pardi, M. Billeter, K. Wüthrich, *J. Mol. Biol.* **1984**, *180*, 741−751.
[20] M. Nilges, M. J. Macias, M. S. J. O'Donoghue, H. Oschkinat, *J. Mol. Biol.* **1997**, *269*, 408−422.
[21] A. Kharrat, M. J. Macias, T. J. Gibson, M. Nilges, A. Pastore, *EMBO J.* **1995**, *14*, 3572−3584.
[22] M. Llinas, M. P. Klein, *J. Am. Chem. Soc.* **1975**, *97*, 4731.
[23] D. W. Urry, M. M. Long, *CRC Crit. Rev. Biochem.* **1976**, *4*, 1−45.
[24] M. P. Williamson, T. Asakura, in: *Protein NMR Techniques: Protein Chemical Shifts* (Ed.: D. G. Reid), Humana Press, Totowa, New Jersey, **1997**, pp. 60−63.
[25] G. D. Rose, L. M. Gierasch, J. A. Smith, in: *Advances in Protein Chemistry: Turns in Peptides and Proteins* (Eds.: F. Richards, E. D. Cera, D. E. Eisenberg, F. M. Richards), Academic Press, Inc., Chestnut Hill, Massachusetts, **1985**, Vol. 37, pp. 1−107.
[26] E. J. Prenner, A. H. Lewis, R. N. Elhaney, *Biochem. Biophys. Acta* **1999**, *1462*, 201−221.
[27] M. A. Andrade, P. Chacon, J. J. Merelo, F. Moran, *Protein Eng.* **1993**, *6*, 383−390.
[28] D. Mation, M. Ikura, R. Tschudin, A. Bax, *J. Magn. Reson.* **1989**, *85*, 393−399.
[29] R. Koradi, M. Billeter, K. Wüthrich, *J. Mol. Graphics* **1996**, *14*, 51−55.

Received July 30, 2003

